

Canonical Timescales In GRBs—1995

Jay P. Norris

NASA/Goddard Space Flight Center, Greenbelt, MD 20771

Understanding the bimodal duration distribution (dynamic range $> 10^4$) of γ -ray bursts is central to determining if the phenomenon is in fact a singular one. A unifying concept, beyond isotropy and inhomogeneity of the two groups separately, is that bursts consist of pulses, organized in time and energy: wider pulses are more asymmetric, their centroids are shifted to later times at lower energies, and shorter, more symmetric pulses tend to be spectrally harder. Long bursts tend to have many pulses while short bursts usually have few, relatively narrow pulses. Two factors, viewing angle and beaming, may account for pulse asymmetry and the large dynamic range (~ 200) in pulse widths.

A cosmological time-dilation signature, with an expected dynamic range of order two, would be difficult to measure against these large intrinsic variations and low signal-to-noise levels of dimmer bursts. Some statistics (T_{90} , pulse intervals) are particularly sensitive to brightness bias, noise, and apparently minor variations in definition. Also, spectral redshift would move narrower, high-energy emission from dim bursts into the band of observation, constituting a countering effect to time dilation. With analyses restricted to bursts longer than ~ 2 s, tests for time dilation that are constructed to be free of brightness bias have yielded time-dilation factors ~ 2 – 3 , for pulse structures, intervals between structures, and durations.

GRB BIMODAL DURATION DISTRIBUTION

Beyond the isotropy and departure from homogeneity of γ -ray bursts (GRBs), their bimodal duration distribution (1) may be the most defining feature. If we only understood why this phenomenon (or phenomena) has a dynamic range of almost five decades in event duration, we might begin to understand GRBs. We do know a few things in connection with the bimodal appearance, enough perhaps to speculate that it reflects a unified phenomenon: Long and short bursts, on either side of the “valley” at ~ 2 s, are separately isotropically distributed (2). There is evidence that both groups are undernumerous at low peak fluxes, compared to the Euclidean expectation in a homogeneously filled space (3), although the best measurement of peak flux for very short bursts is probably yet to be realized. That is, if one truly believes peak flux to be an indicator of distance with some fidelity, then time-tagged event data ($2\text{-}\mu\text{s}$ resolution) should be employed to measure the peak fluxes of short bursts, since pulses in short bursts can be considerably shorter

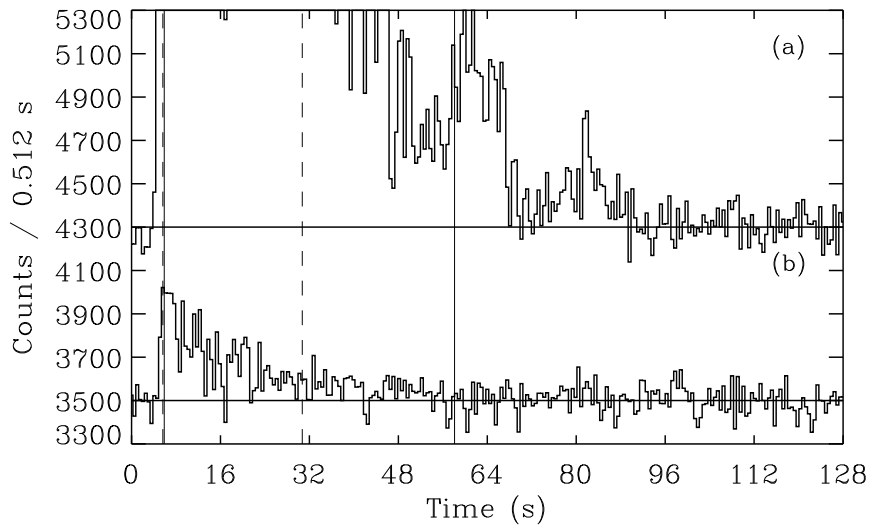


FIG. 1. BATSE burst # 678 with (a) original peak intensity, and with (b) peak intensity reduced to $1400 \text{ counts s}^{-1}$ and variance from the background interval of a dim burst added. The t_5 and t_{95} points are shown as solid (a) and dashed (b) lines, determined from 4σ threshold above background on timescales up to 16 s.

than the shortest (64-ms) timescale on which peak fluxes are tabulated in the BATSE 3B catalog.

Other indicators of kinship are found when the time profiles are examined in detail. Both short and long bursts consist of pulses, that are organized in time and energy, as discussed in the “Pulse Paradigm” section below (4,5). In terms of spectral softening and asymmetry, pulses in short bursts appear to be carbon copies of pulses in long bursts, except that they are, on average, compressed by a factor of ~ 20 . A possible difference between the two groups is that long bursts tend to have many pulses, whereas short bursts often have just a few major pulse structures (6). If the GRB phenomenon is singular, then “telescoping” distributions – in pulse width, pulse interval, and number of pulses per burst – may explain the valley and bimodal appearance (6,7). Short bursts do tend to be spectrally harder (8). But in general, bursts tend to soften as they progress, as demonstrated convincingly by Ford et al. (9). Thus, the softer event-averaged spectra of long bursts may be a matter of the radiation transfer of later pulses being affected by prior burst history.

Establishing duration measurements in a brightness-independent manner is desirable. As illustrated in Figure 1, one can either have accurate durations for bright bursts, or estimations for all bursts (to some threshold) which are relatively free of brightness bias. Figure 1 depicts BATSE trigger # 678 with (a) original peak intensity, and with (b) peak intensity reduced to 1400

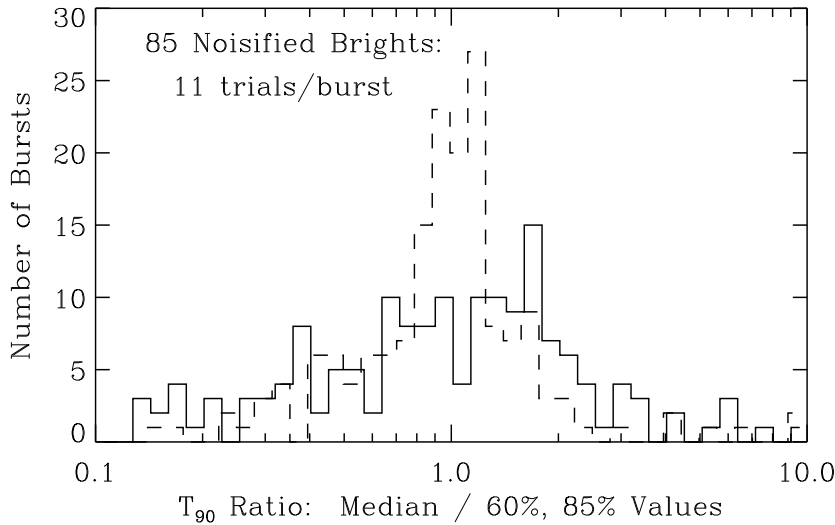


FIG. 2. T_{90} estimations for 85 long, bright bursts, 11 realizations per burst, with peak intensity and signal-to-noise equalized to dim burst level. Solid and dashed histograms are median value divided by 1st and 11th, or by 3rd and 9th ranked values, respectively. Note logarithmic scale on abscissa.

counts s^{-1} and variance from the background interval of a dim burst added. The t_0 and t_{100} points are estimated by seeking the first and last fluctuation, respectively, to exceed the 4σ level above background. For the original peak intensity profile, due to the structure near bin $T = 60$ s, T_{90} is almost twice as long as that for the dimmed and noise-equalized profile. Since for the 3B durations, t_0 and t_{100} points were determined by eye and at original peak intensity and signal-to-noise (s/n) levels, one may conclude that durations of bright bursts are fairly accurately estimated, but that those of dim bursts are underestimated. Since backgrounds are necessarily fitted to the original time profiles, there will be a tendency, regardless of succeeding steps in a duration measurement procedure, to declare low-intensity portions of the burst to be background intervals. This problem exacerbates the underestimation of dim burst durations, and is particularly difficult to circumvent since it is desirable to specify the background near the burst, thereby more accurately fitting any curvature.

The T_{90} statistic is particularly vulnerable to statistical fluctuations, since the t_5 and t_{95} points are necessarily near the t_0 and t_{100} points, which are ill-defined. Figure 2 illustrates T_{90} estimations for 85 long ($T_{90} > 2$ s) bright bursts (peak flux [256 ms] > 4.6 photons $cm^{-2} s^{-1}$). Eleven realizations were performed per burst, with peak intensity and s/n equalized to dim burst levels as described for Figure 1. Solid and dashed histograms are for the median

value divided by 1st and 11th, or by 3rd and 9th ranked values ($\sim 85\%$ and $\sim 60\%$ confidence, respectively). The spread in T_{90} (note logarithmic scale on abscissa) is attributable in many bursts to low-intensity tails or small outlier structures, which are (de)accentuated by fluctuations present in one run but not in another, and which contribute little to the total counts, but considerably to the total event duration. One must conclude that T_{90} is not a terribly robust and useful statistic. Obviously, T_{50} is influenced by the determination of the t_0 and t_{100} points, but less dramatically so. Notice that minor variations in t_0 and t_{100} will have a much larger relative effect on duration estimates for short bursts.

TIME DILATION

In the early 1980s, upon discerning the quasi-isotropy of the KONUS 11/12 burst localizations, Upendra Desai suggested to me to search for the signature of cosmological time dilation in the KONUS sample (duration distributions were constructed and nothing interesting was found). In the BATSE era, Paczynski (10) and Piran (11) made quantitative predictions concerning time dilation in GRB time profiles, based on the BATSE isotropy picture, integral number-intensity relation, standard cosmology and simple source population assumptions (nonevolving luminosity $[L_{\text{GRB}}]$ and space density $[\eta_{\text{GRB}}]$ functions). Because these assumptions have practically never been found to obtain for other cosmological populations (12,13), we should not be surprised to find in the end that L_{GRB} and/or η_{GRB} evolve with cosmic time (14,15) or that any presently observed time stretching effects anti-correlated with GRB brightness are partly or purely special relativistic manifestations (16).

The timescales on which cosmological time dilation would be observed in GRBs and corresponding methods used to search for the signature are summarized in Table 1. Each timescale and method has its peculiar drawbacks, related to brightness bias; to the necessity of determining and applying a correction for spectral redshift of temporal structure; or to the heterogeneous nature of burst profiles. It is difficult designing sensitive tests to measure a cosmological time-dilation factor, $\text{TDF} = [1+z_{\text{dim}}]/[1+z_{\text{brt}}]$, which may be of order 2–3 (10,11,19,21), when the dynamic range in durations is $> 10^4$, and the dynamic range of pulse-structure widths is $\sim 10^2$.

Assuming that the intrinsic burst process does not evolve with cosmic time, then all timescales in the table, except one, would necessarily be required to manifest equal TDFs after correction for redshift effects. The exception (since η_{GRB} is not guaranteed a constant value) is the timescale between bursts, probed by the number-intensity relation. Several studies (17–21), which take into account brightness-bias effects and energy-dependent narrowing effects arising from redshift have found mutually consistent results for long bursts, thus supporting the cosmological time-dilation interpretation. For short bursts, several difficulties – smaller sample with requisite tempo-

TABLE 1. Timescales for Cosmic Time Dilation in Long Bursts

Phenomenon	Timescale	Method	Primary Complications
Redshift	$\sim 300 \text{ keV}/c$	peak in $\nu F(\nu)$ ^a	spectral shape, bandpass
Pulse widths	$\sim 0.2 - 1 \text{ s}$	pulse fitting	ID'ing true pulses
Pulse Intervals	$\sim 0.3 - 3 \text{ s}$	peak finding	ID'ing true intervals
“Burst Core”	$\sim 2 - 4 \text{ s}$	ACF	width correction
	$\sim 8 - 16 \text{ s}$	peak align	ID'ing peak, width corr.
Durations	$2 - 600 \text{ s}$	T_{50}, T_{90}	brightness bias
Burst Intervals	$\sim 1 \text{ day}$	$\log(N)\text{-}\log(P)$	$\eta_{\text{GRB}}, L_{\text{GRB}}$

^aref: (23)

ral resolution, greater dispersion in relative duration from noise, difficulty of precise measurement of peak flux for pulses shorter than 64 ms – combine to make bias-free analyses more problematic. Recent automated approaches attempt to address these complications (22).

As implied by Figure 1, a primary problem with using event durations to measure time dilation is that virtually all of a bright BATSE burst is easily apprehended by eye, whereas for a relatively dim BATSE burst ($\sim 20 - 100$ times less intense), low-intensity structures are lost in the statistical fluctuations. By constructing two duration distributions for long, bright bursts, with original peak intensity and with peak intensity equalized to that of dim bursts, and then applying a uniform threshold to define t_0 and t_{100} points, we can roughly estimate the degree of brightness bias that must be inherent in the 3B durations. Figure 3 illustrates these two distributions for the T_{90} measure. The distribution with equalized peak intensity is shifted to lower values relative to that for original peak intensity by factors of 1.7 (Gaussian fits), 1.4 (K-S test), or 2.8 (average of ratio of $\log[\text{duration}]$). The corresponding factors for T_{50} are 1.3, 1.2, and 1.7, respectively. These brightness-bias factors will tend to obscure a time-dilation effect of order two. Therefore, careful consideration should be given to nullifying brightness-bias effects when estimating durations.

Two methods have been used to measure the width of the “burst core” – the region near burst peak intensity – often comprising several pulses. These are the peak-alignment method (17,24) and the auto-correlation function (ACF) (19,25). Such methods are widely appreciated to be common-sense approaches to search for time dilation in GRB profiles. Both approaches utilize the region near maximum count rate. The peak-alignment method is a linear sum of peak-normalized profiles, but finding “the” peak in dim bursts and accounting for noise bias at the peak can be problematic. The ACF is a nonlinear combination of the peak region with itself. The peak-finding problem is much ameliorated, but the ACF width is affected by noise in dim bursts. In both methods, the noise problems are addressable by equalization of the s/n levels of intensity groups that are being compared (19).

But, concomitant with time dilation is redshift: the temporal structure as-

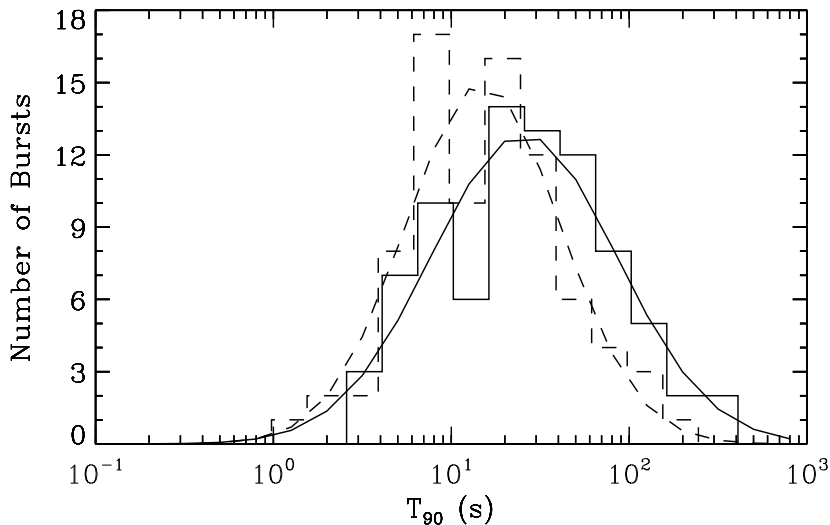


FIG. 3. T_{90} duration distributions and Gaussian fits for long, bright bursts, with original peak intensity (solid) and with peak intensity equalized to that of dim bursts (dashed). The distribution for dimmed bursts is shifted to lower values, illustrating the brightness bias against “seeing” the entirety of dim bursts.

sociated with each energy range is shifted to lower energies in the observer’s frame of reference. Since GRB temporal structures are narrower at higher energy, this redshift-dependent narrowing of temporal structure competes with cosmological time dilation. Moreover, in “stack and average” approaches, *dilation of intervals between pulses* is included, and this diminishes the original effect one wishes to measure, dilation of temporal structure. Thus, width corrections must be applied in order to compare with expectations of any cosmological modelling. The combined correction for redshift and interval dilation is largest for the ACF statistic, and practically as large for the peak-alignment method (19).

Figure 4 is a schematic illustration of these two effects combined. The top panel represents a burst at zero redshift. The tallest pulse has been located to be used in some “burst core” measure of time dilation. The bottom panel is the same burst coming from a redshift of unity, $TDF = 2$. The solid curve shows the time-dilation effect. Note that there is more space between pulses. The dashed curve includes the degree of pulse narrowing for a redshift of approximately unity. Combined, interval dilation and pulse narrowing constitute a large width correction to the observed time-dilation measure. Dilation of intervals between pulses was not properly taken into account in previous treatments (17,25). An estimation is made of the combined correction, using 16-channel data, by redshifting and time-dilating profiles of bright bursts,

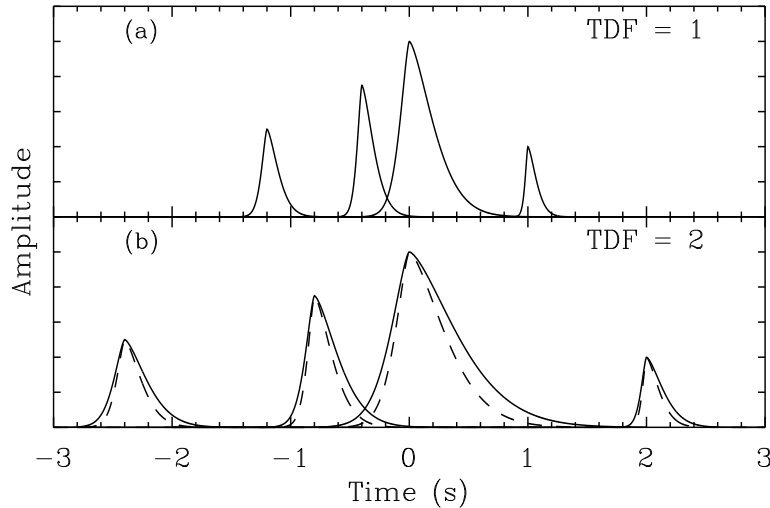


FIG. 4. Schematic of dilation of pulses and intervals, and energy-dependent narrowing of pulse structure. (a) Burst at zero redshift. (b) Same burst from redshift of unity (TDF = 2); solid curve shows time-dilation effect on pulses and intervals; dashed curve includes pulse narrowing for redshift of ~ 1 . Combined, interval dilation and pulse narrowing necessitate large time-dilation correction for methods which average time profiles or ACFs.

yielding correction factors of ~ 1.4 (peak-align) and ~ 1.6 (ACF), assuming for example, an actual TDF of ~ 2.5 between bright and dim bursts (19). Both approaches yield consistent corrected TDFs, but only constrain the allowable TDF to lie within the range 2–3.

Note that since bursts are shorter at higher energy (9), a correction analogous to that required to compensate for pulse narrowing is necessary for duration measures of time dilation (21). If the true TDF were 2 (or 3), then the correction factor is of order 1.10 (or 1.25). Thus the time-dilation measure for durations is less affected by redshift than those for the “burst core.”

For one potential measure of time dilation, $[3B \text{ fluence}]/[3B \text{ peak flux}]$, three adjustments would be necessary to correct for weighting of the counts by the redshifted photon energy (in fluence but not flux), narrowing of pulse structure, and shorter durations at higher energy. In fact, this measure would yield uncorrected TDFs *less than unity* for dim bursts. In addition, systematic errors in fluence for dim bursts may arise in the process of background fitting.

One might think that measurements of intervals between pulse structures would be most free of systematics and energy-dependent effects, and thus would yield an observed TDF closest to the actual TDF. But some consideration shows that related problems will plague interval measures of time dilation: Intervals between pulses in bright bursts are much more clearly de-

lineated than in dim bursts. As a time profile is dilated, additional, shorter intervals can appear near the limit of resolution of the data. Also, narrower temporal structures at higher energy redshifted into the observation band will result in deeper minima between peaks, more readily sensed by a thresholding algorithm. The latter two effects will tend to result in a smaller observed TDF as two new, shorter intervals arise from bifurcation of one interval.

Procedures have been devised in attempts to overcome these problems (20,26). Rendering all burst profiles to the same s/n level helps defeat the brightness-bias problem. Wavelet- (or Fourier-) denoising of profiles (34) may be performed to diminish the frequency of insignificant peaks. Approximate calibration of systematic effects arising from time dilation and redshift can be achieved by stretching and redshifting bright bursts at original resolution, and performing measurements on all bursts at several times the original resolution. Some attempts have been made to devise good automated tests of interval dilation, but these methods are still somewhat immature. Distributions of pulse widths and intervals were measured by Davis using a semi-automated approach (27). Scargle has developed a fully automated pulse-fitting algorithm that should allow model variations to be tested for short bursts (22).

If the time dilation observed in bursts is cosmological, then *intervals between bursts* would also be time-dilated, and this would be reflected in the number-intensity distribution since the observable is a “density rate” (e.g., bursts $\text{yr}^{-1} \text{Gpc}^{-3}$) – observed volumes and time intervals at high redshift are larger than in the comoving frame of the burst. These General Relativistic effects are correctly taken into account in some (14,25,28,29), but not all, recent literature. However, the possibilities of cosmological source-density and/or luminosity evolution, or nonstandard cosmology, introduce considerable latitude into the modelling of redshift parameter space, enough so to make problematic – or at least questionable – the derivation of useful constraints vis-a-vis inclusion of time-dilation measurements. Also, some treatments so far have (inconsistently) analyzed results of time-dilation measurements for long bursts (> 2 s) and the number-intensity distribution for all bursts. Very interestingly, it may be that a GRB luminosity function is implied by the fact that dim, soft-spectrum events appear to follow a number-intensity relation rather close to a $-3/2$ power law (30,31,1). This could have important ramifications for many aspects of GRB analyses and modelling.

PULSE PARADIGM

In the hard X-ray/low energy γ -ray portion of the spectrum – now well-mapped by BATSE – GRBs appear to be composed of pulses which are organized in time and energy. This observation is important because pulses must reflect the “atoms” of the emission process, the details upon which we must ultimately rely to understand much of the high-energy physics, even if bursts are eventually observed in other wavebands. A global characteristic to be ex-

plained by physical modelling is that the envelopes of burst time profiles tend toward asymmetry (longer decays) (32). This tendency appears to extend to shorter timescales within a burst (33), that is, to pulses.

Figure 15 of ref. (5) schematically illustrates the range of pulse shapes that are found in relative isolation, where we do not have to worry too much about blended, overlapping shapes distorting the statistics. Shown are the approximate extremes of pulse shapes and spectral dependences of pulses that have been fitted in bright bursts longer than ~ 2 s. The range of pulse behavior is seen to go from {symmetric, narrow, with negligible lag between energy bands, and tending to be spectrally harder} to {asymmetric with longer decays, wider, low energy lagging high energy, and spectrally softer}. Similar patterns are found in a preliminary study of pulses in short bursts using time-tagged event data, but with the pulse timescale telescoped by a factor of ~ 20 compared to that for long bursts. Pulses in short bursts are more often completely separated from their neighbors (frequently a short burst appears to comprise only a few pulses), and perhaps for this reason the pulse paradigm appears cleaner for them (see Figure 2 of ref. (4)). Automated pulse fitting and denoising approaches may clarify this picture (22,34,35).

Some bursts clearly exhibit the pulse paradigm throughout the whole event. For example, trigger # 2083 consists of two main pulses, both wide, with longer decays than rises, and with the pulse centroids shifted to later times at low energy relative to high energy. Trigger # 678 (shown in Figure 1, but truncated and with insufficient resolution!) has a large number of spiky pulses, each one (as far as can be disentangled) symmetric down to a timescale of 16 ms with no shift in centroid with energy (33). Thorough analyses need to be conducted to determine to what degree this pattern prevails in bursts.

The pulse asymmetry/centroid lag pattern extends across a range in pulse widths from ~ 10 ms to ~ 1 s. It would seem that a variation in boost factor, Γ , cannot entirely account for the range of pulse widths, since then a comparable range in spectra would result. But a combination of dynamic range in Γ and variation in some geometrical factor, e.g., viewing angle, may account for the range of pulse widths. In such a scenario, viewing angle would be related to degree of pulse asymmetry, which is correlated with pulse width in long bursts (for physical modelling of pulses, see refs. (36–39)). This would also be consistent with the observation that short bursts are, on average, spectrally harder than long bursts (8), and with the slight trend for more symmetric, narrower pulses to be harder (5). The observed spectral hardness of a pulse, however, must also be a function of intrinsic beaming factor and position within a burst (radiation transfer dependent on preceding pulses) since we know that bursts tend to soften as they progress (9).

In conclusion, I wish to point out that, once again at a GRB conference (last time, Stanford 1984), the temporal domain was given first billing. Clearly this is more in tribute to BATSE's capabilities for recording bursts' time histories, allowing us to examine more closely their chaotic nature, rather than to our ability to understand the phenomenon. But let us not forget that the burst

physics is written in large proportion in their temporal evolution.

It is a pleasure to acknowledge innumerable enlightening conversations with with many GRB aficionados, including especially Jerry Bonnell, Ed Fenimore, Robert Nemiroff, and Jeffrey Scargle.

REFERENCES

1. C. Kouveliotou, *et al.*, these proceedings.
2. M.M. Briggs, *et al.*, ApJ **459**, in press (1995).
3. C.A. Meegan, these proceedings.
4. J.P. Norris, Ap Space Sci **231**, 95 (1995).
5. J.P. Norris, *et al.*, ApJ **459**, in press (1996).
6. J.P. Norris, *et al.*, in *Gamma-Ray Bursts 1993*, (AIP **307**: New York), 172 (1994).
7. V. Wang, these proceedings.
8. C. Kouveliotou, *et al.*, ApJ **413**, L101 (1993).
9. L.A. Ford, *et al.*, ApJ **439**, 307 (1995).
10. B. Paczynski, Nature **355**, 521 (1992).
11. T. Piran, ApJ **389**, L45 (1992).
12. V. Trimble, in *Gamma-Ray Bursts 1993*, (AIP **307**: New York), 717 (1994).
13. C. Hazard, in *The Space Distribution of Quasars*, (ASP: San Francisco), 170 (1991).
14. J.M. Horack, *et al.*, these proceedings.
15. J.M. Horack, R.S. Malozzi, T. Koshut, ApJ in press (1996).
16. J.J. Brainerd, ApJ **428**, L1 (1994).
17. J.P. Norris, *et al.*, ApJ **424**, 540 (1994).
18. J.P. Norris, *et al.*, ApJ **439**, 542 (1995).
19. J.P. Norris, *et al.*, these proceedings (peak-align, ACF).
20. J.P. Norris, *et al.*, these proceedings (peak intervals).
21. J.T. Bonnell, *et al.*, these proceedings.
22. J.D. Scargle, *et al.*, these proceedings.
23. R.S. Malozzi, *et al.*, ApJ **454**, 597 (1995); and these proceedings (1996).
24. I.G. Mitrofanov, Ap Space Sci **231**, 103 (1995).
25. E.E. Fenimore and J.S. Bloom, ApJ **453**, 25 (1995).
26. J. Neubauer and B. Schaefer, these proceedings.
27. S.P. Davis, *Ph.D. thesis*, The Catholic University of America (1995).
28. E. Cohen and T. Piran, ApJ (1995).
29. R.J. Nemiroff, *et al.*, these proceedings.
30. G. Pizzichini, talk given at COSPAR, Hamburg, (1994); and these proceedings.
31. B.M. Belli, Ap Space Sci **231**, 43 (1995).
32. B. Link, R.I. Epstein, and W.C. Priedhorsky, ApJ **408**, L81 (1993).
33. R.J. Nemiroff, *et al.*, ApJ **423**, 432 (1994).
34. C.A. Young, D.C. Meredith, and J.M. Ryan, these proceedings.
35. A. Lee, E. Bloom, and J.D. Scargle, these proceedings.
36. E.E. Fenimore, C.D. Madras, and Nayakshin, preprint (1996).
37. R. Mochkovitch, V. Maitia, and R. Marques, Ap Space Sci **231**, 441 (1995).
38. N.J. Shaviv, Ap Space Sci **231**, 445 (1995).
39. R. Sari and T. Piran, these proceedings.